Filopodial Calcium Transients Promote Substrate-Dependent Growth Cone Turning

Timothy M. Gomez,*†‡ Estuardo Robles,‡ Mu-ming Poo,§ Nicholas C. Spitzer

Filopodia that extend from neuronal growth cones sample the environment for extracellular guidance cues, but the signals they transmit to growth cones are unknown. Filopodia were observed generating localized transient elevations of intracellular calcium ($[Ca^{2+}]_i$) that propagate back to the growth cone and stimulate global Ca^{2+} elevations. The frequency of filopodial Ca^{2+} transients was substrate-dependent and may be due in part to influx of Ca^{2+} through channels activated by integrin receptors. These transients slowed neurite outgrowth by reducing filopodial motility and promoted turning when stimulated differentially within filopodia on one side of the growth cone. These rapid signals appear to serve both as autonomous regulators of filopodial movement and as frequency-coded signals integrated within the growth cone and could be a common signaling process for many motile cells.

Growth cone filopodia are sensory/motor protrusions that first detect changes in the molecular milieu during axon pathfinding (*1*–*3*). Activation of receptors at their tips by interaction with ligands may generate signals that are transmitted back to the growth cone where they are transduced into changes in motility, but both the identity of these signals and whether they regulate filopodial movement directly are unknown. Although slow spontaneous changes in $[Ca^{2+}]_i$ within growth cones have been imaged at 0.1 Hz (*4*, *5*), here we analyzed fast Ca^{2+} dynamics within individual filopodia of cultured *Xenopus* spinal neurons (*6*) by high-speed (8 Hz) confocal imaging of magnified regions of Fluo-4 loaded growth cones (*7*). Most filopodia (55 ± 14%) of neurons grown on poly-D-lysine (PDL) generated brief Ca^{2+} transients (317 ± 85 ms) during 30-s imaging periods (Fig. 1, A and B) (n = 22 filopodia from seven growth cones); active filopodia generated transients at 9.2 ± 1.1 min^{-1}. Ca^{2+} transients detected by ratiometric imaging of Fluo-4 and Fura-Red fluorescent signals (n = 9) (*8*, *9*) (Fig. 1, C and D) (movie 1, *10*) ruled out artifactual fluorescence elevations due to movement or volume changes. Ca^{2+} elevations occurred locally at the tip or along the length of a filopodium and spread to the growth cone with no apparent decrement at 12.5 ± 0.6 μm/s (n = 12) (Fig. 1, E and F) (movie 2, *10*), consistent with either propagated surface entry or intracellular diffusion in a weakly buffered environment (*11*). Filopodial transients appeared similar to growth cone transients (*4*, *5*) in that they depended on Ca^{2+} influx through non–voltage-gated channels, but they were distinct because they were not amplified by Ca^{2+} release from internal stores (Fig. 1G).

To determine the dependence of fast Ca^{2+} transients on molecules that regulate neurite outgrowth, $[Ca^{2+}]_i$ was imaged in filopodia of neurons grown on eight different substrates (*12*). Transient frequency varied from one substrate to another whereas duration and amplitude were similar (Fig. 2A) (Web table 1, *10*), indicating that these Ca^{2+} elevations could provide a specific signaling mechanism in growth cone filopodia. Growth cones did not generate global Ca^{2+} transients on tenascin-C (TN), fibronectin (FN), or vitronectin (VN), indicating that on certain substrates local filopodial transients are not sufficient to produce global elevations (Web table 1, *10*). In physiological extracellular Ca^{2+}, the frequency of fast local transients was highest on TN and declined as the TN concentration ([TN]) was lowered (Fig. 2A inset), suggesting that TN stimulates transient production.

Because extracellular matrix (ECM) components, cell adhesion molecules, and artificial substrates stimulate Ca^{2+} transients in filopodia, Ca^{2+} entry could be activated by multiple receptor types. To determine whether a particular class of receptor is sufficient to generate these fast Ca^{2+} transients, we examined the role of β1 integrin receptors that bind many ECM proteins and trigger Ca^{2+} fluctuations (*7*, *13*). The tripeptide sequence arginine-glycine-aspartate (RGD), contained in many ECM molecules including TN (*14*) and recognized by a subset of integrins (*15*), is sufficient to stimulate adhesion and Ca^{2+} influx in non-neuronal cells (*16*). Soluble RGDS (S, serine) elevated $[Ca^{2+}]_i$ in growth cones (Fig. 2B) and increased mean filopodial Ca^{2+} transient frequency from 2.8 ± 0.4 to 4.3 ± 0.8 min^{-1} ($P < 0.05$; n = 26 active and inactive filopodia from seven growth cones). The effects of RGDS were specific because the non–integrin binding peptide RGES (E, glutamate) neither elevated $[Ca^{2+}]_i$ nor altered filopodial transient frequency and antibodies that block the function of β1 integrins (*17*) prevented RGDS-mediated Ca^{2+} elevations. In addition to its effects on the frequency of filopodial Ca^{2+} transients, RGDS evoked transients involving larger regions in the growth cone veil (36%, n = 11) (Fig. 2, C and D) (movie 3, *10*). These findings show that engagement of integrins on neuronal growth cones can activate Ca^{2+} influx and oscillations and suggest that integrin clusters (*18*, *19*) may be the sites of fast local Ca^{2+} transients.

Integrins promote Ca^{2+} influx and adhesion, which lead to increased cell attachment, spreading, and migration (*15*). To determine whether the frequency of fast local Ca^{2+} transients regulates filopodial motility, we measured the lifetime from initiation to retraction of filopodia (*20*, *21*) of growth cones growing on three concentrations of TN that elicit varying frequencies of Ca^{2+} transients (Fig. 2A inset). As the [TN] increased, the average filopodial lifetime also increased, whereas the average axon length decreased. The effect of TN is Ca^{2+}-dependent because blocking local transients with the Ca^{2+} chelator BAPTA reduced filopodial lifetimes (Fig. 3A). Regulation of filopodial lifetime by Ca^{2+} transients could be due to effects on the actin cytoskeleton (*22*) or adhesion through increased integrin affinity or clustering (avidity) (*13*). To test whether Ca^{2+} transients regulate integrin avidity, β1 integrin clustering was examined before and after chelation of Ca^{2+} with BAPTA during the time when filopodial lifetimes are reduced (*23*, *24*). Blocking endogenous filopodial Ca^{2+} transients with BAPTA had no detectable effect on integrin clustering at filopodial tips (Fig. 3, B and C). However, localized Ca^{2+} transients were consistently initiated at sites of punctate integrin clusters (15/15 clusters from 4 growth cones) (Fig. 3, D and E) (Web fig. 1, *10*), suggesting that they stabilize filopodia through integrin activation.

To determine whether Ca^{2+} transients generated in filopodia promote global growth cone transients, we exploited differences in transient frequencies evoked by laminin (LN) and tissue culture plastic (TC). Because growth cones exhibit a higher frequency of

Department of Biology and Center for Molecular Genetics, University of California, San Diego, La Jolla, CA 92093, USA.

*To whom correspondence should be addressed. E-mail: tmgomez@facstaff.wisc.edu

†Present address: Department of Anatomy, University of Wisconsin Medical School, Madison, WI 53706, USA.

‡These authors contributed equally to this work.

§Present address: Department of Molecular and Cell Biology, University of California, Berkeley, CA 94720, USA.

both local and global Ca^{2+} transients on TC than LN, we investigated the distance at which Ca^{2+} dynamics change as growth cones encounter a LN-TC border (*25*, *26*). The frequency of Ca^{2+} transients in growth cones on LN increased as they approached TC, suggesting that filopodial contact with TC is sufficient to induce global Ca^{2+} changes (Web fig. 2A, *10*). The signals promoting global Ca^{2+} transients may be local Ca^{2+} transients because these elevations occurred at a higher frequency within individual filopodia that project onto TC compared with LN (*27*). To investigate whether filopodial input stimulates the production of global Ca^{2+} transients, global transient frequency was measured in growth cones at this boundary in the presence of 100 nM cytochalasin D to disrupt actin filaments. In the absence of filopodia, the frequency of these transients did not increase until growth cones were within 5 μm of the border (Web fig. 2A, *10*). Because Ca^{2+} transients precede growth cone turning in vivo (*28*), we analyzed whether they induce axon turning at a LN-TC border in vitro. Most axons turned to remain on LN when transients were allowed, where-

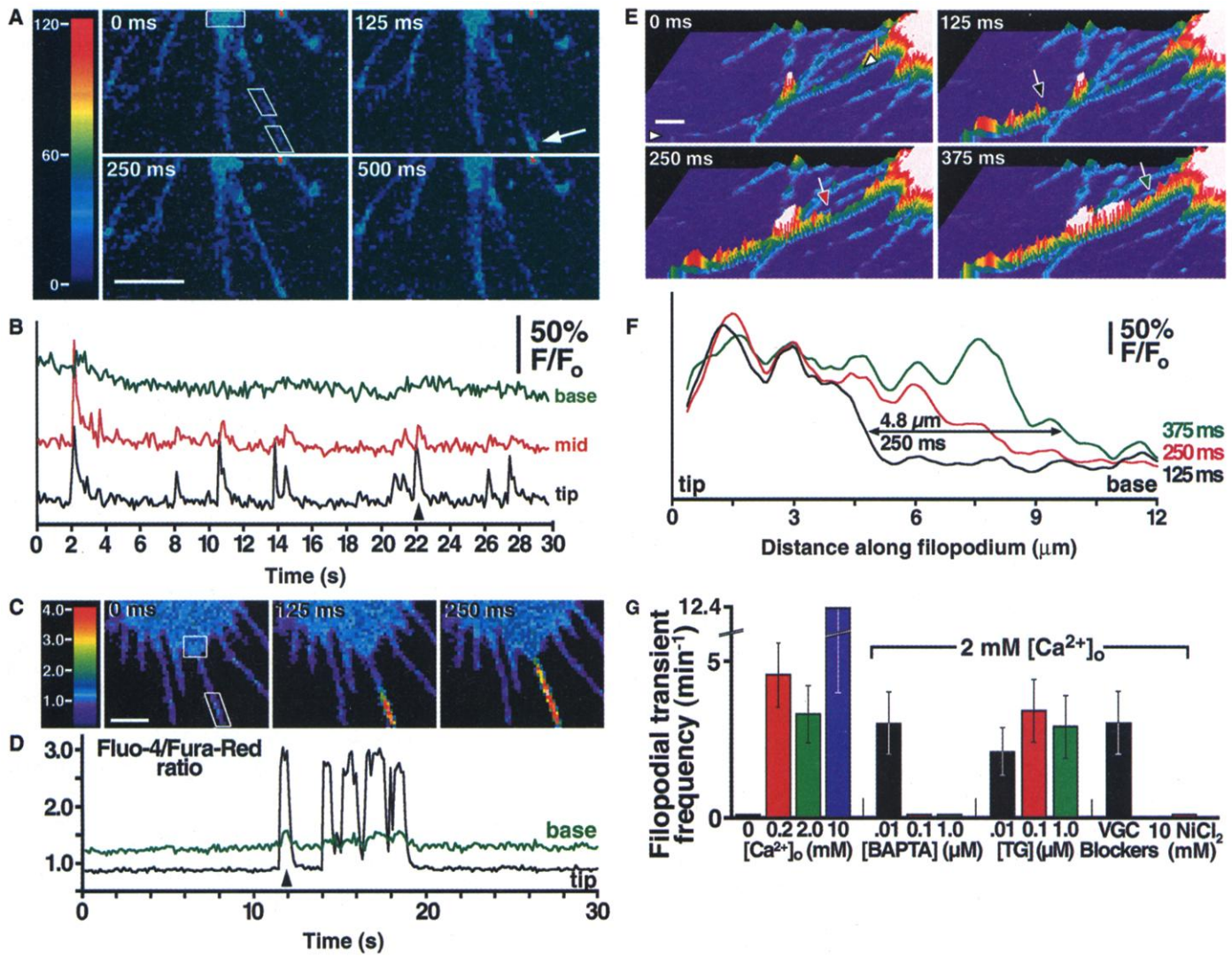

Fig. 1. Spontaneous filopodial Ca^{2+} transients visualized by high-speed imaging of Fluo-4 fluorescence. (**A**) Time-lapse pseudocolor confocal images of Fluo-4 loaded filopodia. Regions selected for quantification at the tip, middle, and base of one filopodium are shown at 0 ms. A local Ca^{2+} transient at the tip occurs at 125 ms (arrow). Fluorescence intensity is coded on a linear pseudocolor scale. (**B**) Normalized fluorescence changes within regions of this filopodium captured at 125-ms intervals. Ca^{2+} transients occur at high frequency at the tip and move proximally toward the growth cone. Arrowhead indicates transient visualized in (A). F/F_0 indicates Fluo-4 fluorescence (F) relative to baseline fluorescence (F_0). (**C**) Pseudocolor ratio images of filopodia loaded with Fluo-4 and Fura-Red. (**D**) Fluorescence ratio increases within regions of the filopodium in (C) demonstrate that these transients are not due to artifacts of movement or volume changes. Note that elevated Ca^{2+} initiated at the tip causes a small elevation of Ca^{2+} at the distal region of this growth cone (base). Arrowhead indicates transient shown in (C). (**E**) Pseudocolor profile images show that elevated Ca^{2+} (colored arrows) moves from tip to base of this filopodium within 375 ms. (**F**) Fluorescence along the filopodium in (E) normalized to resting levels [line-scan between white arrowheads in 0-ms panel in (E)] and smoothed with a five-point moving average. The velocity of propagation is 19.2 μm/s. Synchronous fluctuations are artifacts due to scanning at high zoom. (**G**) Ca^{2+} transients in filopodia on tissue culture plastic are generated by Ca^{2+} influx through a non–voltage-gated channel and are not affected by store release. Ca^{2+} influx is required because the average transient frequency decreased in reduced $[Ca^{2+}]_o$, and transients were abolished in 0 mM Ca^{2+}, with 10 mM NiCl in the presence of 2 mM Ca^{2+} or by intracellular Ca^{2+} chelation with BAPTA. Filopodial transient frequency was unaffected by voltage-gated Ca^{2+} channel blockers (VGC) (50 μM NiCl, 10^{-7} M nifedipine, 10^{-6} M Ω-conotoxin, and 60 nM Ω-agatoxin) or Ca^{2+} store release with thapsigargin (TG). Neurons were grown on poly-D-lysine (PDL) in 2 mM Ca^{2+} except where indicated and imaged at 12 to 24 hours in culture. $n > 20$ filopodia for each condition. Bar in (A), (C) and (E), 2 μm.

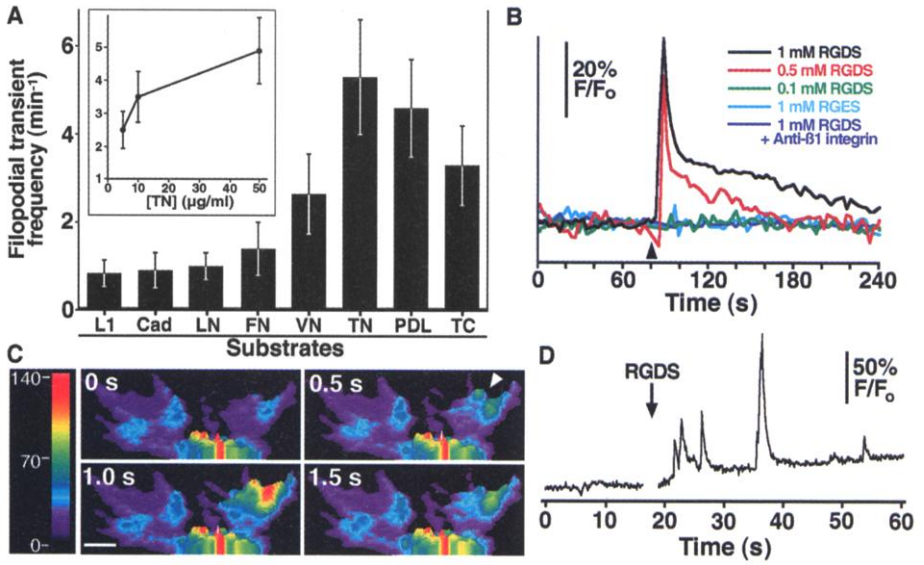

Fig. 2. Frequencies of local filopodial Ca^{2+} transients are regulated by the substrate, in part through integrin receptors. (**A**) The average frequency of transients for all filopodia (including inactive ones) of neurons grown in 2 mM Ca^{2+} on artificial substrates (TC, PDL), cell adhesion molecules [N-cadherin (Cad) and L1], and on ECM components LN, FN, TN, and VN (50 μg/ml). For some substrates (L1, Cad, LN, PDL, and TC) the frequency of global growth cone transients correlated with the local filopodial transient frequency, but no correlation was seen for others (FN, VN, TN). TN stimulated the highest frequency of transients in filopodia, in a dose-dependent manner (inset). $n \geq 10$ filopodia for each condition. (**B**) Soluble RGDS produced a dose-dependent, biphasic elevation of $[Ca^{2+}]_i$ in 75% of growth cones tested (arrowhead; traces are averages from 10 growth cones) and stimulated increased frequency of filopodial and veil transients. Antibodies to β1 integrin did not block spontaneous filopodial Ca^{2+} transients, perhaps due to restricted antibody access. (**C**) Pseudocolor profile images show that elevated Ca^{2+} (arrow) in response to 1 mM soluble RGDS spreads through a growth cone veil in 1 s. Bar, 2 μm. Fluorescence intensity is coded on a linear pseudocolor scale. (**D**) Normalized fluorescence changes within the active veil in (C) captured at 125-ms intervals. Ca^{2+} transients occurred at high frequency after the addition of RGDS (arrow). Gap in trace represents 14 s during application. Neurons in (B) through (D) were grown on TN (5 μg/ml) in 2 mM Ca^{2+}.

as most crossed into TC when global elevations were blocked in either 0.2 mM Ca^{2+} or when all transients were blocked with BAPTA (Web fig. 2B, *10*). These results indicate that when filopodia contact a second substrate, local Ca^{2+} signals spread to the growth cone and stimulate global Ca^{2+} elevations that promote growth cone turning.

To test whether filopodial Ca^{2+} transients on one side of the growth cone are sufficient to promote turning, we examined growth cones at a boundary between high (50 μg/ml) and low (5 μg/ml) TN (*25*). Because growth cones do not generate global Ca^{2+} elevations on TN, Ca^{2+}-dependent turning at a high [TN]/low [TN] border would likely result from differences in the frequency of filopodial Ca^{2+} transients on varying [TN] (Fig. 2A). Seventy-nine percent of axons turned to remain on a low [TN] under control conditions ($n = 28$), whereas only 33% turned when filopodial transients were blocked with 100 nM BAPTA ($n = 27$; $P < 0.002$, Fisher's exact test). To assess differences in local transient frequencies at this border, Fluo-4 loaded growth cones turning away from a high [TN] were imaged (Fig. 4, A and B). Filopodia in contact with a high [TN] exhibited both a higher incidence and frequency (69%, 6.3 ± 0.8 min^{-1}, $n = 26$) of transients compared to those contacting a low [TN] (54%, 4.7 ± 0.4 min^{-1}, $n = 37$, $P < 0.05$). Thus a step-gradient of TN directs axon growth in a Ca^{2+}-dependent manner by stimulating filopodial Ca^{2+} transients on one side of the growth cone.

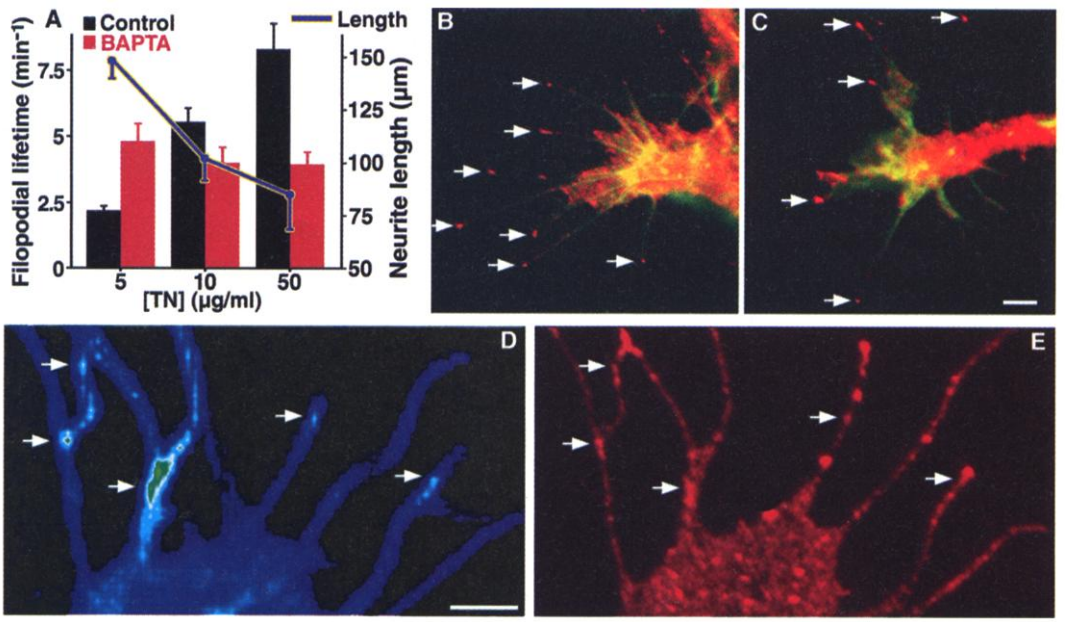

Fig. 3. Local Ca^{2+} transients reduce filopodial motility and slow neurite outgrowth. (**A**) Increased [TN] prolonged filopodial lifetimes and shortened neurite lengths. The effect of [TN] depended on Ca^{2+} transients because 100-nM BAPTA reduced their effects on lifetime ($n \geq 95$ filopodia from three growth cones for each condition) with no effect on resting $[Ca^{2+}]_i$ (*5*). (**B** and **C**) BAPTA-loaded (C) and unloaded control (B) growth cones were double labeled for β1 integrin (red) and actin (green). Neither the proportion of filopodia with integrin clusters at their tip (arrows) (52 versus 44% of 239 total filopodia in 30 growth cones; $P = 0.3$, Fisher's exact test), nor the size of these clusters (0.15 ± 0.01 μm^2 versus 0.16 ± 0.01 μm^2, $n = 114$ total clusters; $P = 0.4$) was significantly different, indicating that Ca^{2+} transients do not affect motility by increasing receptor clustering. (**D** and **E**) Sites of Ca^{2+} transient activity colocalized with β1 integrin clusters. (D) Pseudocolored maximum projection of a 30-s time-lapse sequence encompassing 240 confocal images of a Fluo-4 loaded growth cone. Bright regions indicate areas of Ca^{2+} transient activity (arrows) (Web fig. 1, *10*). (E) The same growth cone now labeled for β1 integrin shows that regions of transient activity occur at sites of β1 integrin clusters (arrows). Bar in (C) indicates unit of measure in (B) and (C), 2 μm; bar in (D) indicates unit of measure in (D) and (E), 2 μm. Neurons were grown on TN (10 μg/ml) in 2 mM Ca^{2+}.

Because different concentrations of TN may affect axon growth in ways unrelated to filopodial Ca^{2+} transients, we focally released caged-Ca^{2+} within filopodia on a homogeneous substrate to test whether local differences in filopodial transient frequencies are sufficient to produce turning (*29*). Growth cones loaded with caged-Ca^{2+} (NP-EGTA) or unloaded controls were positioned so their forward projecting filopodia extended into a 20-μm spot that was pulsed with UV light (310 to 410 nm) for 200 ms at 10-s intervals. Because nonphotolyzed NP-EGTA chelates spontaneous transients due to its low dissociation constant (K_d) (80 nM) (*30*), Ca^{2+} transients were generated only in those filopodia projecting into the spot (Fig. 4, C and D). After 5 to 10 μm of growth, the direction of axon outgrowth was deflected by 37° ± 8° (n = 10) in all growth cones loaded with caged-Ca^{2+}, but only by 14° ± 3° (n = 10) in unloaded controls (Fig. 4, E and K) ($P <$ 0.02). These results show that filopodial Ca^{2+} transients imposed on one side of the growth cone are sufficient to induce turning away from that side.

Our findings indicate that growth cones exhibit spontaneous cytosolic Ca^{2+} signals over a wide range of spatial and temporal domains that have diverse effects on pathfinding behaviors. The amplitudes of Ca^{2+} gradients imposed within the palm of growth cones also regulate attractive or repulsive turning (*31*, *32*). The frequency of Ca^{2+} transients in filopodia depends on substrate type and concentration, underscoring their biological significance. Ca^{2+} elevations detected in isolated filopodia in contact with guidance cues may be initial signaling events necessary for adhesion (*33*). Integrin-mediated Ca^{2+} influx through non–voltage-gated channels seems to contribute to Ca^{2+} signals that result in decreased filopodial motility, possibly by feedback activation of integrins (*13*). Although integrins appear to be sufficient to stimulate Ca^{2+} transients, they are not necessary given activation by non–integrin binding substrates. Filopodial Ca^{2+} transients are similar to other types of elemental signaling processes such as vesicular transmitter release (*34*) and Ca^{2+} puffs and sparks (*35*), because they can be summed to produce global actions on certain substrates. The autonomous effects of local Ca^{2+} signals on filopodial motility and substrate-specific ability to induce global elevations of $[Ca^{2+}]_i$ together provide versatile control of growth cone behavior.

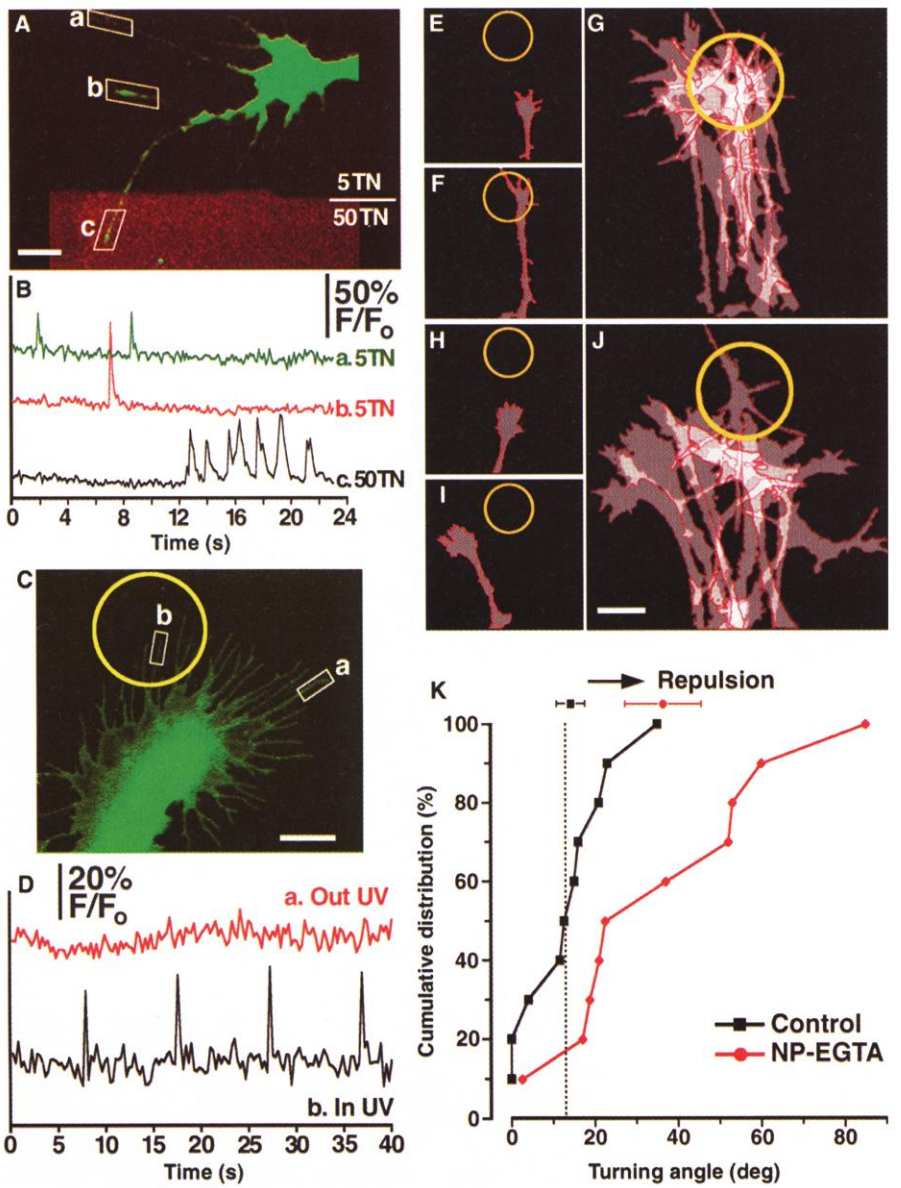

Fig. 4. Local filopodial Ca^{2+} transients regulate turning. (**A**) Fluo-4 loaded growth cone turning at a border between high and low [TN]. Border is identified by TRITC fluorescence (50 μg/ml TN). Filopodia on either side of the boundary were monitored for Ca^{2+} transient activity (boxes). Bar, 5 μm. (**B**) Normalized fluorescence changes within regions of the filopodia in (A) captured separately at 125-ms intervals. The frequency of Ca^{2+} transients is higher in the filopodium on 50 μg/ml TN than those on 5 μg/ml TN. (**C**) Fluo-4/NP-EGTA double-loaded growth cone placed adjacent to a spot within which filopodia are exposed to UV pulses (yellow circle) whereas those outside are not. Bar, 10 μm. (**D**) Normalized fluorescence changes within regions of the filopodia in (C) captured sequentially at 125-ms intervals. Ca^{2+} elevations at a frequency of 6 min^{-1} are generated only in filopodia within the spot. (**E** through **K**) Fast Ca^{2+} transients imposed in filopodia on one side of a growth cone promote turning to the other side. Unloaded control [(E) through (G)] and NP-EGTA loaded [(H) through (J)] growth cones at the onset of UV pulses [(E) and (H)] and after 30 min growth toward the spot [(F) and (I)]. (G) and (J) Superimposed profiles of unloaded control growth cones (G) and those loaded with NP-EGTA (J) after 5 to 15 μm of growth toward a region exposed to pulsed UV light at 6 min^{-1} (yellow circles). In only one instance did a growth cone loaded with caged-Ca^{2+} penetrate the pulsed region. Bar in (J) indicates unit of measure in (E), (F), (H), and (I), 20 μm; bar in (J) indicates unit of measure in (G) and (J), 10 μm. (K) Cumulative distribution of turning angles for growth cones loaded and unloaded with caged-Ca^{2+}. Vertical dashed line represents the average turning angle of growth cones loaded with caged-Ca^{2+} but not exposed to UV light. Neurons in (C) and (E) through (J) were grown on 50 μg/ml LN in 2 mM Ca^{2+}. (G) and (J), n = 10.

References and Notes

1. S. B. Kater, V. Rehder, *Curr. Opin. Neurobio.* **5**, 68 (1995).
2. T. P. O'Connor, J. S. Duerr, D. Bentley, *J. Neurosci.* **10**, 3935 (1990).
3. C. B. Chien, D. E. Rosenthal, W. A. Harris, C. E. Holt, *Neuron* **11**, 237 (1993).
4. T. M. Gomez, D. M. Snow, P. C. Letourneau, *Neuron* **14**, 1233 (1995).
5. X. Gu, N. C. Spitzer, *Nature* **375**, 784 (1995).
6. X. Gu, E. C. Olson, N. C. Spitzer, *J. Neurosci.* **14**, 6325 (1994).
7. For Ca^{2+} imaging, neurons were loaded with 2 to 5 μM Fluo 4-AM [with 0.01% pluronic acid/0.1% dimethyl sulfoxide (DMSO) in modified Ringer's solution (MR) (*3*); Molecular Probes] for 1 hour at 20°C, rinsed, and imaged at frequencies of 0.06 to 8 Hz on Bio-Rad MRC 600 argon laser or MRC 1024 krypton/argon laser confocal systems. Eight-Hz imaging was performed with the MRC 1024 mounted on an Olympus BX70 upright

microscope using either a 60× water (NA 0.9) or 100× oil (NA 1.4) objective. An acquisition box of 100 pixels by 40 pixels was used to increase collection speed and zoomed to achieve pixel sizes between 0.2 and 0.4 μm. Reduced speed Ca^{2+} imaging (0.06 to 1 Hz) used for RGD experiments (RGDS and RGES from Sigma) and imaging of global growth cone transients was performed on the MRC 600 mounted on a Zeiss upright microscope using a 764 pixel by 512 pixel collection box and a 40× Fluor (NA 1.2) oil objective. For all experiments, laser power was attenuated to 1 to 10% of maximum using neutral density filters. Loose coverslips with adherent neurons were inverted for use with oil objectives by first sealing them on a coverslide with high-vacuum grease (Dow Corning). Inlet and outlet ports were left when necessary for exchange of solutions.

8. P. Lipp, E. Niggli, *Cell Calcium* **14**, 359 (1993).
9. For combined Fluo-4/Fura-Red imaging, neurons loaded with 5 μM Fluo-4–AM and 5 μM Fura-Red–AM (in 0.01% pluronic acid) were excited with the 488-nm laser line of the MRC 1024 and images were collected at both 522 ± 35 and at ≥585 nm wavelengths. Fluorescence was quantified and changes were normalized to baseline using MetaMorph (Universal Imaging) or NIH Image (W. Rasband, NIH) software; events exceeding 10% of baseline fluorescence were scored as filopodial transients. Statistical significance was determined using Student's *t* test unless otherwise noted, and variance is reported ±SEM.
10. Web figures 1 and 2, Web table 1, and three Quicktime movies are available at *Science* Online at www.sciencemag.org/cgi/content/full/291/5510/1983/DC1.
11. N. L. Allbritton, T. Meyer, L. Stryer, *Science* **258**, 1812 (1992).
12. Cultures of dissociated spinal neurons and neural tube explants were prepared from stage 20 to 22 *Xenopus* embryos. Cells were grown at 20°C in MR containing 2 mM Ca^{2+} (*3*) on untreated tissue culture plastic or on various biological substrates coated onto tissue culture plastic or acid-washed glass coverslips, usually at saturating concentrations (LN, FN, VN, and Poly-D-lysine from Sigma; TN from Gibco).
13. M. A. Schwartz, M. D. Schaller, M. H. Ginsberg, *Annu. Rev. Cell Dev. Biol.* **11**, 549 (1995).
14. M. A. Bourdon, E. Ruoslahti, *J. Cell Biol.* **108**, 1149 (1989).
15. R. O. Hynes, *Cell* **69**, 11 (1992).
16. M. G. Coppolino *et al.*, *Nature* **386**, 843 (1997).
17. D. S. Sakaguchi, K. Radke, *Brain Res. Dev. Brain Res.* **97**, 235 (1996).
18. P. C. Letourneau, T. A. Shattuck, *Development* **105**, 505 (1989).
19. P. W. Grabham, D. J. Goldberg, *J. Neurosci.* **17**, 5455 (1997).
20. D. Bray, K. Chapman, *J. Neurosci.* **5**, 3204 (1985).
21. For analysis of filopodial lifetimes and for Ca^{2+} photorelease studies, neurons were labeled with green fluorescence protein–actin (GFP-actin) to enhance visualization of filopodia. Two individual blastomeres at the eight-cell stage were injected with 1 to 5 ng of capped GFP-actin mRNA (mMessage machine, Ambion). Filopodial lifetime measurements were made on growth cones from loaded (1 hour, 100 nM BAPTA AM; Molecular Probes), and unloaded cultures on 5, 10, or 50 μg/ml TN. Motile growth cones were selected and imaged at 15-s intervals for 30 min with the MRC 600 using a 100× oil objective. Lifetimes were measured as described (*20*) using NIH Image software, except that filopodia present at the beginning of the observation period were included for analysis.
22. M. Lu, W. Witke, D. J. Kwiatkowski, K. S. Kosik, *J. Cell Biol.* **138**, 1279 (1997).
23. Combined β1 integrin/phalloidin labeling was performed immediately after Fluo-4 imaging and rapid perfusion of cold fixative through the coverslip chamber. Mouse primary antiserum to β1 integrin (1:50, AB 8C8; Developmental Studies Hybridoma Bank) was applied for 1 hour followed by 1:20 Oregon Green Phalloidin with secondary antibody (1:250, Alexa Fluor 568 goat antibody to mouse; Molecular Probes) for 1 hour. Immunofluorescent images of actin filaments and β1 integrin receptors were captured using the MRC 1024. Integrin receptor clusters were defined on the basis of fluorescence intensity, and their areas were quantified using NIH Image software.
24. T. M. Gomez, F. K. Roche, P. C. Letourneau, *J. Neurobiol.* **29**, 18 (1996).
25. Substrate boundaries were created by protecting regions of culture dishes with Sylgard (Dow Corning) strips as described (*26*), except that boundaries were identified by including 5% tetramethyl rhodamine isothiocyanate (TRITC) (Molecular Probes) with the first substrate coated.
26. T. M. Gomez, P. C. Letourneau, *J. Neurosci.* **14**, 5959 (1994).
27. Average filopodial transient frequency was 2.7 ± 0.7 min^{-1} on TC and 1.3 ± 0.3 min^{-1} on LN. Data are from six filopodia of three growth cones on each substrate imaged at 1 Hz.
28. T. M. Gomez, N. C. Spitzer, *Nature* **397**, 350 (1999).
29. For Ca^{2+} photorelease experiments, GFP-actin expressing spinal cord explants were plated onto LN-coated glass coverslips. After 6 to 18 hours in culture, neurons were loaded with 2.5 μM caged-Ca^{2+} (NP-EGTA AM; Molecular Probes) for 1 hour then rinsed in MR. Motile growth cones were positioned with their leading edge 10 μm in front of a 20-μm spot and imaged at 15-s intervals for approximately 30 min with the MRC 600 using a 100× oil objective. A programmable shutter (Uniblitz) pulsed this spot with 310- to 410-nm ultraviolet light filtered from a 100-W mercury lamp for a duration of 200 ms every 10 s. The direction of neurite growth was measured from the center of the leading edge to middle of the neurite at the base of the growth cone using NIH Image. The maximum difference in the angle of neurite growth between 5 to 15 μm of growth was scored. Neurites with a net extension of <5 μm over the 30-min period were not included. Photorelease of Ca^{2+} in selected filopodia was tested using non–GFP expressing neurons loaded with 2.5 μM Fluo-4 and NP-EGTA.
30. G. C. Ellis-Davies, J. H. Kaplan, *Proc. Natl. Acad. Sci. U.S.A.* **91**, 187 (1994).
31. J. Q. Zheng, *Nature* **403**, 89 (2000).
32. K. Hong, M. Nishiyama, J. Henley, M. Tessier-Lavigne, M. Poo, *Nature* **403**, 93 (2000).
33. T. B. Kuhn, C. V. Williams, P. Dou, S. B. Kater, *J. Neurosci.* **18**, 184 (1998).
34. P. Fatt, B. Katz, *J. Physiol.* **117**, 109 (1952).
35. S. Koizumi *et al.*, *Neuron* **22**, 125 (1999).
36. We thank I. Hsieh, A. Marnik, and J. Kaufman for technical assistance and K. Kalil and P. Letourneau for comments on the manuscript. We thank K. Yamada (National Cancer Institute) for providing antibodies that block the function of β1 integrin, V. Lemmon (Case Western Reserve) for providing L1 and NCAD, and J. Hegmann (Basel) for providing the GFP-actin construct. Supported by a NIH NINDS fellowship to T.M.G. and by grants to N.C.S.

11 October 2000; accepted 31 January 2001

Requirement for the SLP-76 Adaptor GADS in T Cell Development

Jeff Yoder,[1] Christine Pham,[2,3,4] Yoshie-Matsubayashi Iizuka,[3] Osami Kanagawa,[4] Stanley K. Liu,[5] Jane McGlade,[5] Alec M. Cheng[2,3,4]*

GADS is an adaptor protein implicated in CD3 signaling because of its ability to link SLP-76 to LAT. A GADS-deficient mouse was generated by gene targeting, and the function of GADS in T cell development and activation was examined. $GADS^-$ $CD4^-CD8^-$ thymocytes exhibited a severe block in proliferation but still differentiated into mature T cells. $GADS^-$ thymocytes failed to respond to CD3 cross-linking in vivo and were impaired in positive and negative selection. Immunoprecipitation experiments revealed that the association between SLP-76 and LAT was uncoupled in $GADS^-$ thymocytes. These observations indicate that GADS is a critical adaptor for CD3 signaling.

The development and function of T cells are regulated by signaling through the CD3 complex, which serves both the pre–T cell receptor (pre-TCR) and the TCR [(*1*) and references therein]. Cross-linking of CD3 induces protein tyrosine phosphorylation in a wide range of proteins. Among these phosphorylation targets are two adaptor proteins, LAT and SLP-76, which function in a coordinated fashion to activate a diverse set of signaling proteins (*2–5*). The critical function of SLP-76 and LAT is supported by the observation that mice lacking SLP-76 or LAT exhibit an absolute block in early thymocyte development (*6–8*).

The function of SLP-76 is dependent on its association with LAT (*9–13*). This association is mediated by an adaptor known as GADS, which contains two SH3 domains flanking a SH2 domain and a linker region. GADS associates constitutively with SLP-76 through the binding of the GADS SH3 domain, and is recruited to LAT through binding of its SH2 domain to phosphotyrosine motifs on LAT upon TCR activation (*9–11*, *13*). Besides GADS, Grb2 and possibly Grap are also implicated as adaptors for SLP-76 (*4*). Because mutant T cells or primary mast cells lacking LAT demonstrate reduced phosphorylation of SLP-76 upon receptor activa-

[1]Medical Scientist Training Program; [2]Center for Immunology; [3]Division of Rheumatology, Department of Medicine; [4]Department of Pathology and Immunology; Washington University School of Medicine, St. Louis, MO 63110, USA. [5]Hospital for the Sick Children, University of Toronto, Toronto, Canada.

*To whom correspondence should be addressed. E-mail: acheng@im.wustl.edu